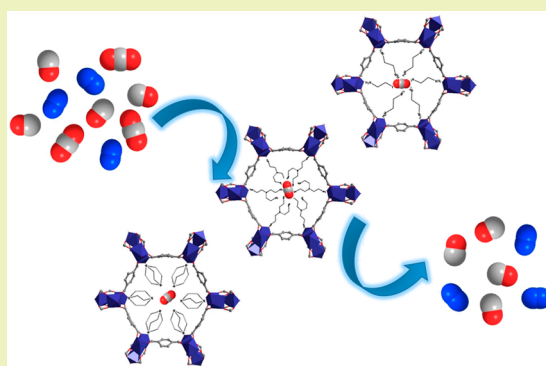


Amine-Grafted MIL-101(Cr) via Double-Solvent Incorporation for Synergistic Enhancement of CO₂ Uptake and SelectivityRuiqin Zhong,^{*,†,§} Xiaofeng Yu,^{†,‡,§} Wei Meng,^{‡,§} Jia Liu,^{‡,§} Chenxu Zhi,[†] and Ruqiang Zou^{*,‡,§}[†]State Key Laboratory of Heavy Oil Processing, China University of Petroleum, Beijing, No. 18 Fuxue Road, Changping District, Beijing 102249, China[‡]Beijing Key Laboratory for Theory and Technology of Advanced Battery Materials, Department of Materials Science and Engineering, College of Engineering, Peking University, No. 5 Yiheyuan Road, Haidian District, Beijing 100871, China

Supporting Information

ABSTRACT: Recent research on the amine-grafted metal–organic frameworks has obviously spurred intriguing application prospects in the field of CO₂ capture; however, few of them focused on the synthetic approach, which directly determines their structural stabilities for the application. This work explores a double-solvent incorporation strategy to rapidly squeeze the molecule-level amines into the cavities of MIL-101(Cr) without any framework destruction of MOFs. Tris(2-aminoethyl) amine (TAEA), ethylenediamine (ED) and triethylene diamine (TEDA) were employed to obtain TAEA@MIL-101(Cr), ED@MIL-101(Cr) and TEDA@MIL-101(Cr), respectively. Notably, the CO₂ uptake of TAEA@MIL-101(Cr) could be 1.5 times as high as that of pure MIL-101(Cr) at 273 K with a superhigh adsorption heat. Most importantly, the CO₂/CO selectivity of TAEA@MIL-101(Cr) was drastically increased, which was 103 times higher than that of MIL-101(Cr). The experimental and theoretical simulation results indicated the different adsorption mechanism of CO₂ in the three amine-grafted MIL-101(Cr) materials.



KEYWORDS: Metal–organic framework, Postsynthetic modification, Organic amine, CO₂ capture, CO₂/CO separation

INTRODUCTION

With the development of global industrialization and the explosive growth of the population, excessive consumption of fossil fuel sharply increases the content of CO₂ in atmosphere, which will break the global carbon balance, and cause a series of ecological problems.^{1–3} In addition, the 90% hydrogen in refinery is derived from light hydrocarbon steam reforming technology. The syngas (H₂ and CO) produced by this technology often contains impurities of CO₂, which will directly affect the energy efficiency during further utilization, and thus the capture and separation of CO₂ is of great significance for syngas. The CO₂/H₂ separation is relatively easy, thanks to nonpolarity of H₂, and therefore the key step for CO₂ separation from syngas lies in the CO₂/CO separation. At present, the technologies and methods⁴ of carbon dioxide adsorption and separation mainly include the following aspects: absorption method,^{5–7} low temperature separation method,⁸ membrane separation method,^{9–11} and adsorption method^{12–14} etc. However, these methods have inherent drawbacks. For example, the absorption of CO₂ by amine solution demonstrates high separation selectivity, but the energy cost of regeneration is high and the solution will severely corrode equipment. In terms of adsorption method, it is crucial to select a suitable adsorbent material for capture and separation of CO₂. The porous materials used for gas adsorption separation mainly include

activated carbon, mesoporous silica and molecular sieves. Although there are a lot of adsorbent materials used for CO₂ capture and separation, the CO₂ adsorption capacity of these materials is not high,¹⁵ mainly due to the weak interaction between materials and CO₂. It is urgent to find suitable solid adsorbent materials.

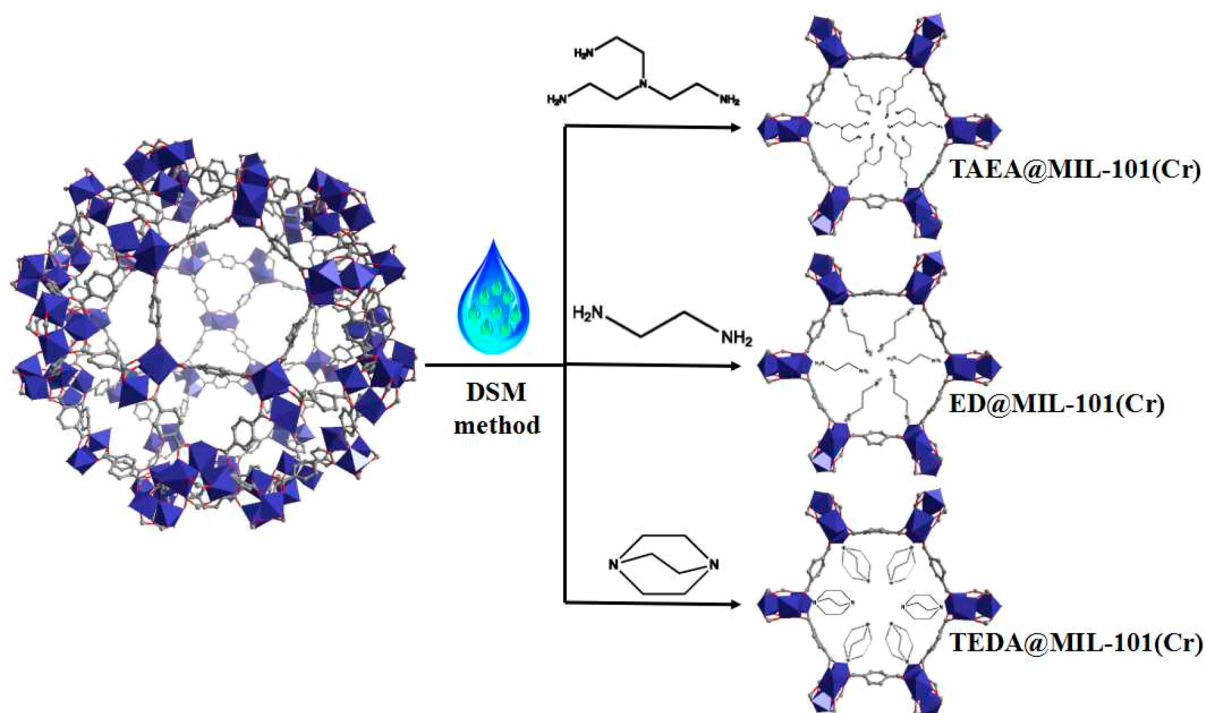
Metal–organic frameworks (MOFs) as a family of organic–inorganic hybrid porous materials¹⁶ are composed of metal cations or metal clusters as nodes and organic ligands as linkers.^{17,18} Different from other adsorbent materials with limited controllability for tuning their gas adsorption/separation performance, MOFs not only have high specific surface area, tunable pore size/shape and pore volume, but also can be easily modified.¹⁹ It is for the reason that these materials in the field of CO₂ adsorption is favored.^{17,20–23} Gas separation mechanism mainly includes the diffusion and thermodynamic adsorption. Therefore, the design of materials must take into account the gas molecular dynamics and electronic properties.²⁴ Some zeolitic imidazolate framework (ZIF) structures have exhibited high efficiency for the separation of CO₂/CO via molecular sieving effect,²⁵ which is mainly attributed to the appropriate pore

Received: July 25, 2018

Revised: October 10, 2018

Published: October 30, 2018

Scheme 1. Schematic Diagram of Grafting MIL-101(Cr) with Three Different Amines



apertures of ZIFs with the size falling into the range of dynamic diameters of CO (0.376 nm) and CO₂ (0.33 nm). However, it remains a big challenge to finely tune the pore apertures of MOFs.²⁶ Nevertheless, the differences in the electronic properties (quadrupole, dipole moment and polarizability) of CO₂ and CO could be also utilized to realize their separation. The chemical modification of pore surface can effectively change the surface electronic properties of materials, and then improve the selectivity of CO₂ adsorption.^{27–30} The surface chemical modification mainly includes the direct synthesis method^{31–34} and the post synthesis modification method, yet sometimes the direct synthesis method cannot obtain the MOFs material with high crystallinity.³⁵ At present, the postsynthetic modification mainly includes impregnation method,^{36–40} grinding method and reflux method,^{30,41–43} but these methods are unable to control the loading of amines, and attachment of amine molecules to external surface of MOFs unavoidably occurred.³⁵ It is very easy to lose the amine molecules on the surface of MOFs, leading to the decrease of the adsorption capacity of the material during cycled operation, which means the stability of the composite is not satisfactory. More importantly, some polar molecules like amines often partially decompose the host framework of MOFs under unsuitable preparation procedure, which leads to dramatic loss of surface area and porosity of MOF materials.

In this paper, the MIL-101(Cr)⁴⁴ was selected as the porous material, mainly because it has not only high specific surface area and mesoporosity but also a high concentration of open metal sites (~3.0 mmol/g^{45,46}), as well as high chemical stability. Up to now, there are quite a few reports on amine-modified MIL-101(Cr) for CO₂ capture, which exhibit remarkable improvement of CO₂ uptakes.^{41,47–54} For example, Jiang group and Zhou group have developed various solvent impregnation methods to modify different organic amines to MIL-101(Cr) or derivative,^{53,54} and these materials have demonstrated excellent CO₂ adsorption properties. In addition, few reports focused on

the accurate loading control of amine molecules without the structural decomposition of the host frameworks during the synthetic procedures. Herein, we employed an efficient post synthesis modification approach, double-solvent method (DSM), which can effectively avoid the adhesion of a large number of guest molecules on the external surface of the material.⁵⁵ According to polar molecules and nonpolar solvent (*n*-hexane), the guest molecules can be more easily squeezed into the polar pore of MIL-101(Cr) under the action of capillary force (Scheme 1). Using this method, we successfully modified three kinds of organic amine molecules to MIL-101(Cr), and significantly improved both CO₂ uptakes and the selectivity of CO₂/CO separation.

EXPERIMENTAL SECTION

Materials and Methods. *Synthesis of MIL-101(Cr) and amine@MIL-101(Cr) (amine = TAEA, ED, TEDA).* The MIL-101(Cr) samples were synthesized according to previous report without using hydrofluoric acid.⁵⁶ 0.2 g of Cr(NO₃)₃·9H₂O, 0.83 g of terephthalic acid and 20 mL of deionized water were blended and sonicated for 20 min. Then the suspension was transferred to the autoclave with Teflon liner and kept in an oven at 218 °C for 18 h. When the reaction mixtures returned to room temperature, the products were separated by centrifuge (10,000 r/min, 10 min) and washed several times with water, methanol and acetone. The solids obtained by centrifugation were placed into 20 mL of DMF for ultrasonic treatment of 10 min, and transferred to the 70 °C thermostat overnight. After cooling to room temperature, solid was obtained by centrifugation, and repeatedly washed with methanol and acetone. Finally, the products were vacuum-dried at 150 °C for 10 h.

For all amine@MIL-101(Cr) samples, the amount of loaded amine was slightly more than 3 mmol/g, which depends on the open metal site concentration of MIL-101(Cr).

Synthesis of TAEA@MIL-101(Cr). The synthesized MIL-101(Cr) is activated in a vacuum at 150 °C for 10 h, then 50 mL of hexane is directly poured into activated MIL-101(Cr) (500 mg). After treated in an ultrasonic bath for 20 min, the *n*-hexane dispersion of MIL-101(Cr) was gradually added with 0.25 mL TAEA using the syringe pump within

half an hour under vigorous stirring, and then the mixture was sealed for 4 h, after which the container was left open until all hexane is evaporated. The obtained green powder is activated for 5 h under vacuum at 150 °C, to remove the residual hexane solvent and the TAEA molecules attached to the external surface of the materials.

Synthesis of ED@MIL-101(Cr). The syntheses processes are similar to that of TAEA@MIL-101(Cr), in which 0.1 mL ED were employed in replacement of TAEA.

For TEDA@MIL-101(Cr), 0.33g TEDA was dissolved in 0.52 mL of water, and then the solution was added to MIL-101(Cr).

Materials Characterization. Powder X-ray diffraction (PXRD) patterns for the materials were collected on a Rigaku D/max 2400 X-ray diffractometer operating at 40 kV and 100 mA, using Cu K α radiation ($\lambda = 1.5406 \text{ \AA}$). The scanning range was 3°–50° at a rate of 8° per min. Scanning electron microscopy (SEM) images were recorded using a Hitachi S4800 electron microscope to analysis the morphologies of the samples, and transmission electron microscopy (TEM) images were recorded using a Hitachi H9000 electron microscope. Thermogravimetric analyses (TGA), for as-synthesized materials, were carried out on a SDT Q600 analyzer from TA Instruments under a continuous nitrogen flow (100 mL min⁻¹) at a heating rate of 10 °C min⁻¹. Isobaric gravimetric CO₂ sorption cycle test was also collected using SDT Q600 analyzer to examine the regenerability and stability of materials. Elemental analysis (EA) of MIL-101(Cr) and amine@MIL-101(Cr) was performed with Elementar Vario EL CUBE (Germany) analyzer, while metal contents of the samples were detected by inductively coupled plasma atomic emission spectrometry (ICP-AES) on a Thermo IRIS Intrepid. Fourier-transform infrared spectroscopy (FT-IR) spectra were recorded by a Bruker Tensor 27 Fourier transform infrared spectrometer from 400 to 4000 cm⁻¹ (KBr pellets).

Gas Adsorption Measurements. All the gases (N₂, CO₂, CO) used in this study were of ultrahigh purity (99.999%). Nitrogen adsorption isotherms at 77 K were performed on Quantachrome Autosorb-IQ gas adsorption analyzer in a liquid nitrogen bath. The CO₂ and CO sorption isotherms were measured at 273, 293 and 298 K using circulating glycol/H₂O bath, respectively. Before the measurement, about 100 mg of the adsorbent materials was degassed at 150 °C for 10 h in vacuum condition.

Selectivity Calculations of Ideal Adsorbed Solution Theory (IAST). The ideal adsorbed solution theory (IAST)^{57,58} was used to estimate the CO₂/CO separation performance through the single component sorption isotherms, with the detailed procedure shown in Supporting Information. First, the pure component isotherms should be fitted by suitable model. Dual-site Langmuir model was employed to fit the CO₂ adsorption isotherm while single-site Langmuir model for CO adsorption (Figures S4–S19). In this work, the IAST selectivity was calculated based on a CO₂/CO (50/50) mixture at both 273 and 298 K. The detailed calculating procedure of the IAST method has already been established in many published works.¹⁶

Simulations. The interactions between CO₂ and amine grafted MIL-101(Cr) were studied by employing the density functional theory (DFT-D) method⁵⁹ with the PBE (Perdew–Burke–Ernzerhof) function and DNP basis set.⁶⁰ According to crystal structure, an 88-atom model of MIL-101(Cr) has been employed, while three Cr(III) sites have been specially concerned. Two of the three Cr atoms of the model are five-coordinated with O_{carboxyl} from BDC ligand, with a noncoordinative site that can interact with guest molecules. The geometries of the MIL-101(Cr) and amine modified MIL-101(Cr) are calculated before and after CO₂ adsorption.

RESULTS AND DISCUSSION

Structural Analysis of amine@MIL-101(Cr). The images of SEM and TEM show that the MIL-101(Cr) particles have octahedral morphology with clear edges and corners, which is consistent with the literature (Figures 1 and S1).¹⁶ It also indicates that the MIL-101(Cr) synthesized by nonhydrofluoric acid method has comparable quality of crystallinity. As expected, the three kinds of amine modified composite, TAEA@MIL-101(Cr), ED@MIL-101(Cr) and TEDA@MIL-101(Cr) main-

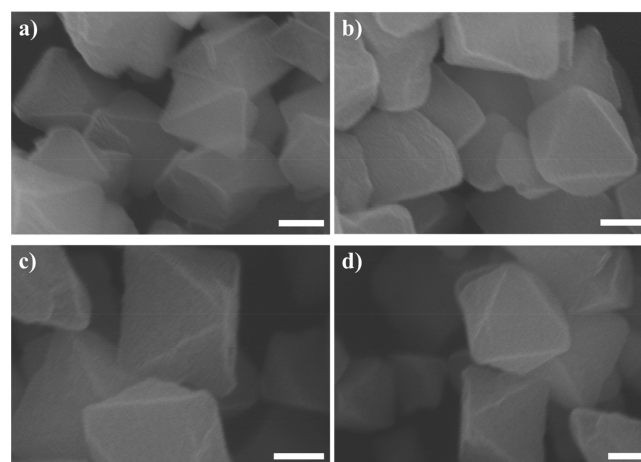


Figure 1. SEM images of (a) MIL-101(Cr), (b) TAEA@MIL-101(Cr), (c) ED@MIL-101(Cr) and (d) TEDA@MIL-101(Cr). Scale bars: 100 nm.

tained the original morphology and the crystal size of MIL-101(Cr), indicating that DSM is a mild and efficient method for modifying amino groups onto MOFs, which at the same time, has little damage to the parent materials.

The PXRD patterns of synthesized MIL-101(Cr) are in good agreement with the simulated one (Figure 2), which implies that

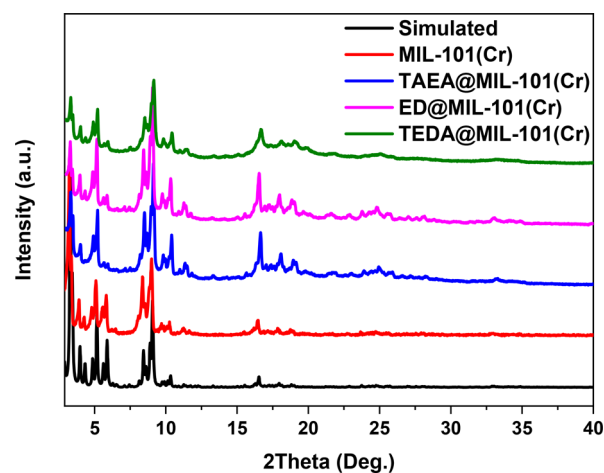


Figure 2. PXRD patterns of MIL-101(Cr), TAEA@MIL-101(Cr), ED@MIL-101(Cr), TEDA@MIL-101(Cr), and the simulated one from crystallographic information file of MIL-101(Cr).

the synthesized materials have high crystallinity and purity. The PXRD patterns of amine modified TAEA@MIL-101(Cr), ED@MIL-101(Cr) and TEDA@MIL-101(Cr) are almost the same as unmodified raw MIL-101(Cr) in both peak positions and relative intensities, illustrating that the modification of materials by three kinds of amines has no influence on the structure of the parent MIL-101(Cr), and the original topology are well maintained.

TGA was employed to evaluate the effect of amine modification on the thermal stabilities of materials. As shown in Figure 3, three kinds of modified materials show the similar form of TGA curves as the original MIL-101(Cr). TAEA@MIL-101(Cr) and TEDA@MIL-101(Cr) demonstrate similar amount of weight loss before 100 °C (about 30%), mainly due to the departure of solvent in the pore of materials. The weight

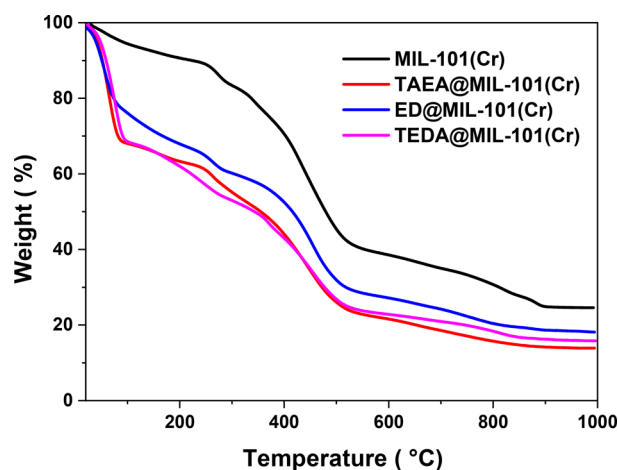


Figure 3. TGA curves of samples.

loss percentage of TAEA@MIL-101(Cr) and TEDA@MIL-101(Cr) is slightly larger than ED@MIL-101(Cr) before 300 °C because of low molecular weight of ED. As for the weight loss steps between 300 and 470 °C, this could possibly be the loss of organic ligand and partial structure collapse. Furthermore, the EA results (see Table S1 in Supporting Information) indicated that three kinds of amine molecules have been appended to the parent MIL-101(Cr) framework according to expected loading percentage (molar ratio of Cr/amine was close to 1 for each modified composite).

The N₂ adsorption/desorption isotherms of the materials were measured at 77 K to investigate the porosity (Figure 4a). As expected, postsynthetic modification of materials will lead to decrease of specific surface area and pore volume. After modification, the pore volume of TAEA@MIL-101(Cr) was reduced from 1.785 to 0.691 cm³ g⁻¹ (Table 1), mainly because TAEA molecules occupy large amount of pore space. Under the same loading, the surface area of TEDA@MIL-101(Cr) (1806.9 m² g⁻¹) and ED@MIL-101(Cr) (1584.6 m² g⁻¹) is much higher than that of TAEA@MIL-101(Cr) (1279.2 m² g⁻¹). The reason could be that the larger TAEA molecules partially block the channels of MIL-101(Cr).

To accurately assess the influence of the loaded amine on the pore of the material, the pore size distribution of the four materials was analyzed (Figure 4b). The main peaks of pore size

Table 1. N₂, CO₂ and CO Adsorption Data of Four Samples

compound	surface area (m ² g ⁻¹)	pore volume (cc g ⁻¹)	CO ₂ uptake at 1 bar mmol g ⁻¹		CO uptake at 1 bar mmol g ⁻¹	
			273 K	298 K	273 K	298 K
MIL-101(Cr)	3483.1	1.785	3.26	1.61	0.59	0.27
TAEA@MIL-101(Cr)	1279.2	0.691	5.05	2.19	0.50	0.06
ED@MIL-101(Cr)	1584.6	0.916	3.93	1.93	0.42	0.09
TEDA@MIL-101(Cr)	1806.9	0.969	3.81	1.65	0.41	0.23

distribution of ED@MIL-101(Cr), TAEA@MIL-101(Cr) and TEDA@MIL-101(Cr) at 1.0–3.5 nm are all significantly reduced, which indicates that the polar guest molecules are preferentially filled into the inner pores of the material under the extrusion of nonpolar solvents. Through careful analysis (see Table S3 in Supporting Information), we obtained that micropore volumes of all modified materials were reduced much more than mesopore volumes, consistent with the greatly decreased BET surface area. The reduction of pore size of three materials manifests that the guest molecules have been successfully grafted to MIL-101 framework.

To further characterize the modified MIL-101(Cr), FT-IR test was performed, and the results are shown in Figure 5. To remove the water molecules in the samples, the three kinds of materials were first treated by vacuum drying at 150 °C for 12 h. Because the three amine molecules are volatile, this treatment can effectively remove the organic amine molecules attached to the external surface of the materials. Through comparison of the infrared spectra of organic amine and MIL-101(Cr), three amine@MIL-101(Cr) samples maintained the original characteristic peaks of MIL-101(Cr).

From Figure 5a, The characteristic vibration peaks (~3300 cm⁻¹) of -NH₂ are not clearly observed in TAEA@MIL-101(Cr), mainly due to that the structure of MIL-101(Cr) contains many hydroxyl groups, and the strong hydroxyl peaks cover up the -NH₂ vibrational peaks. But the apparent -C-N peak is found at 1030 cm⁻¹, hence confirming the existence of TAEA molecule in the MIL-101(Cr) channels. In ED@MIL-

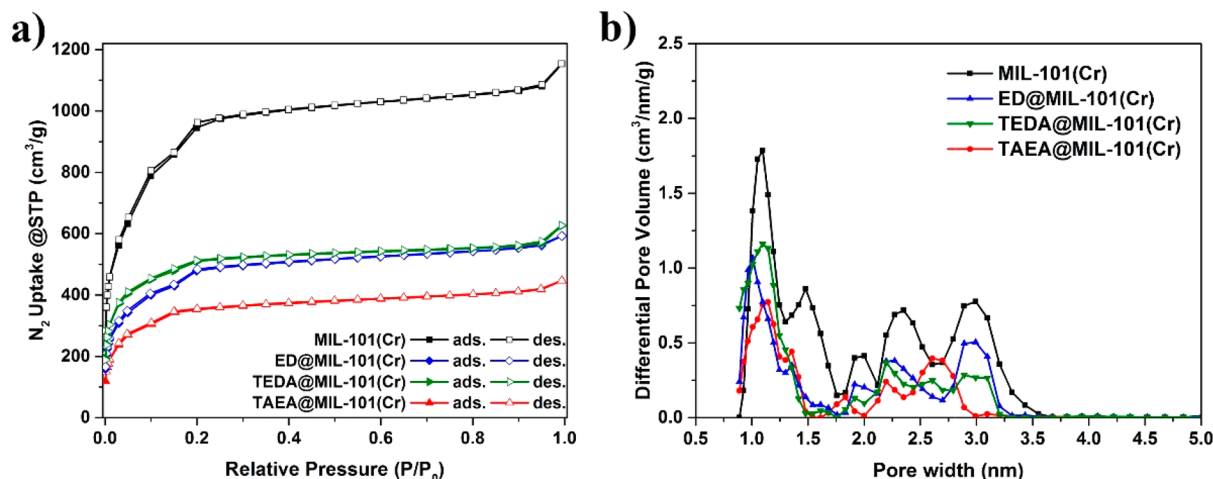


Figure 4. (a) N₂ adsorption isotherms at 77K and (b) pore size distribution curves.

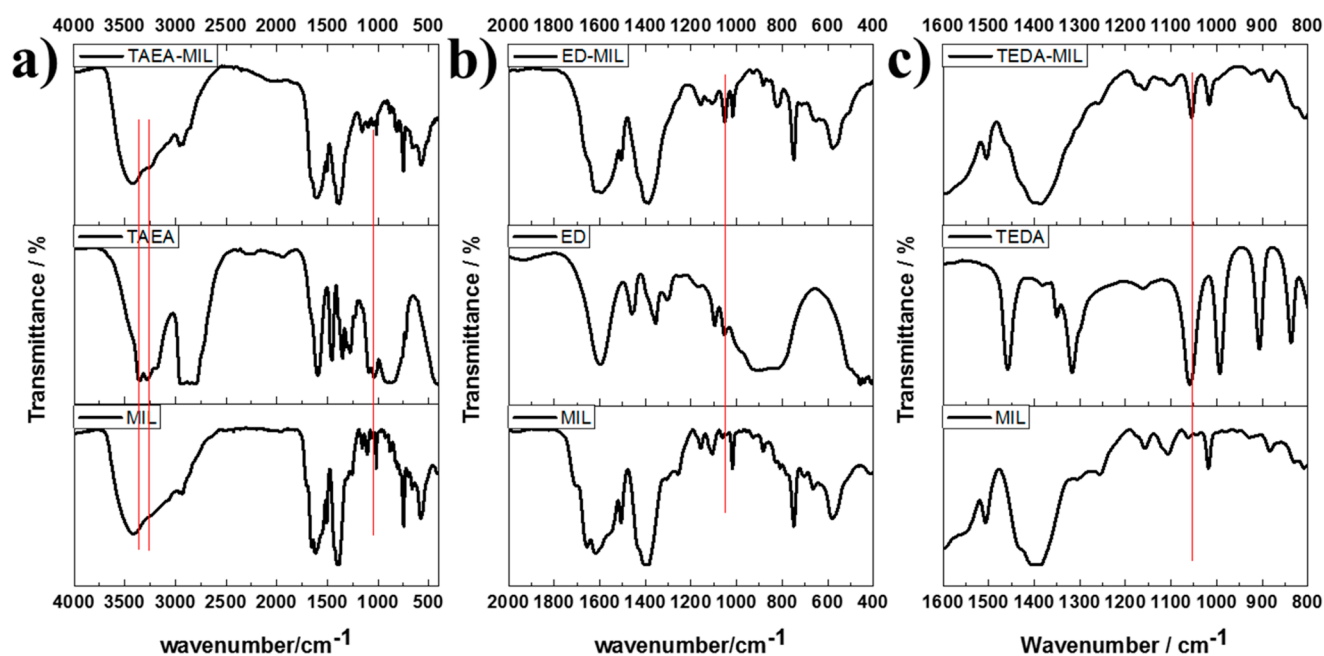


Figure 5. FT-IR results of (a) TAEA@MIL-101(Cr), (b) ED@MIL-101(Cr) and (c) TEDA@MIL-101(Cr).

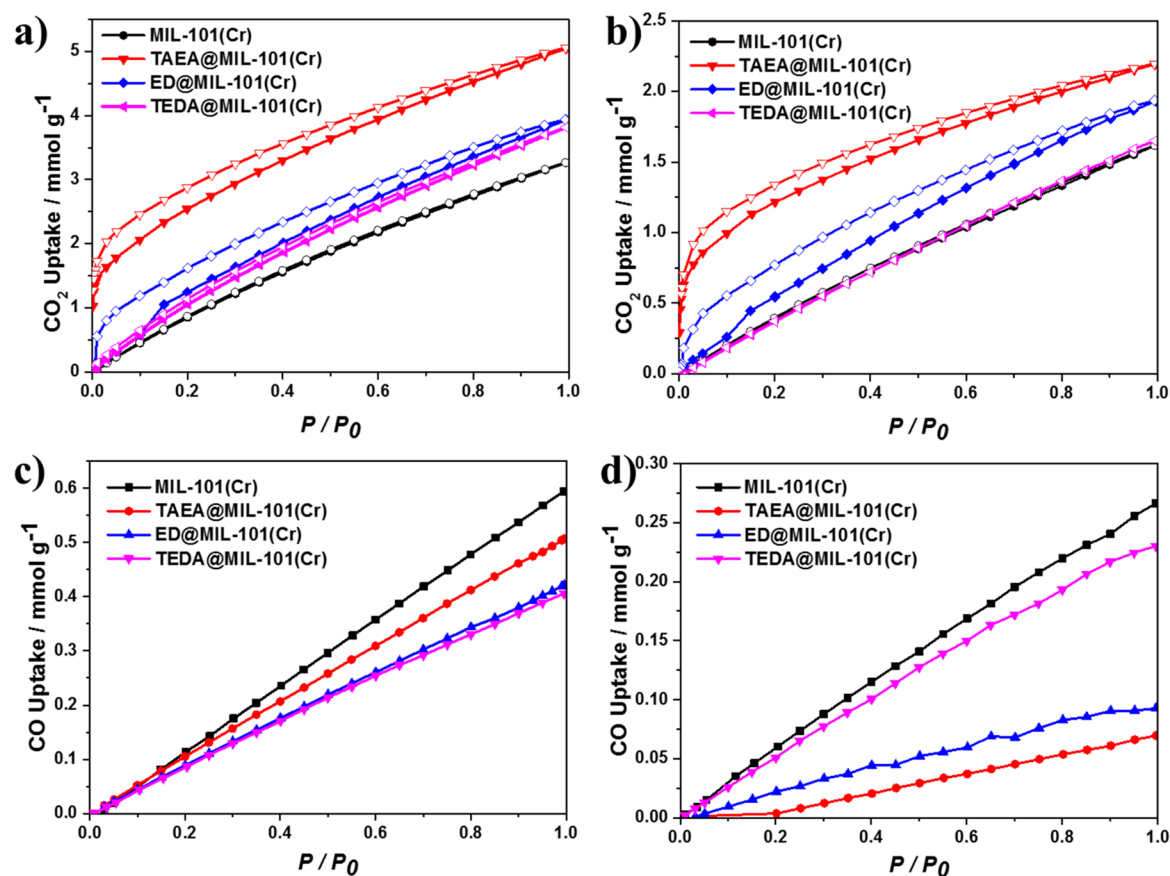


Figure 6. Gas adsorption properties of (a) CO₂ adsorption isotherms at 273 K, (b) CO₂ adsorption isotherms at 298 K, (c) CO adsorption curve at 273 K and (d) CO adsorption curve at 298 K.

101(Cr) and TEDA@MIL-101(Cr), there are still strong $-C-N$ vibrational peaks, and thus three kinds of organic amine molecules have been successfully introduced into MIL-101(Cr) framework.

Gas Adsorption Performance of amine@MIL-101(Cr).

The CO₂ and CO adsorption isotherms at 273 and 298 K are shown in Figure 6 (and 293 K in Figure S3). The results of CO₂ and CO sorption data for MIL-101(Cr), TAEA@MIL-101(Cr), ED@MIL-101(Cr) and TEDA@MIL-101(Cr) at 273 and 298

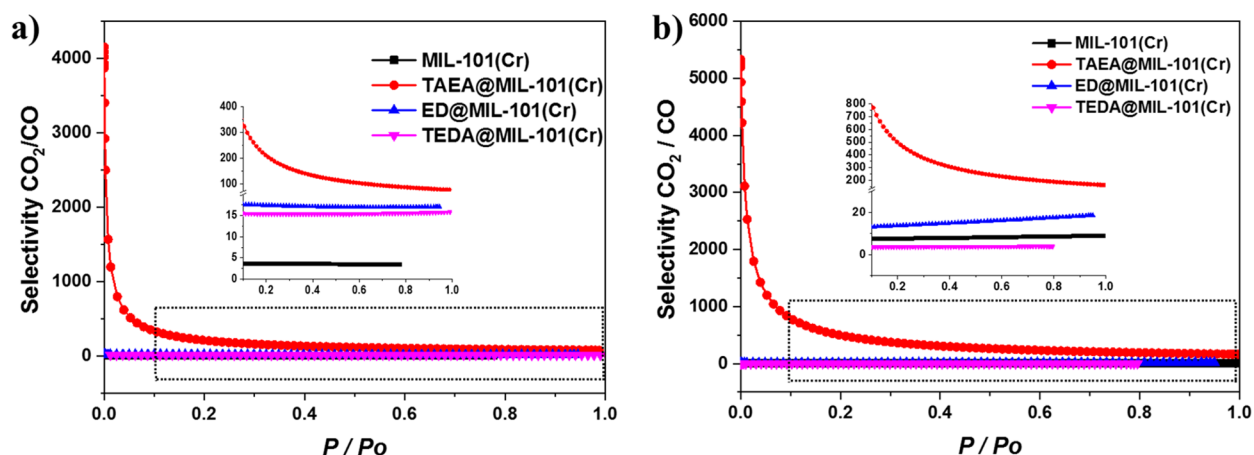


Figure 7. CO₂/CO selectivity at (a) 273 K and (b) 298 K.

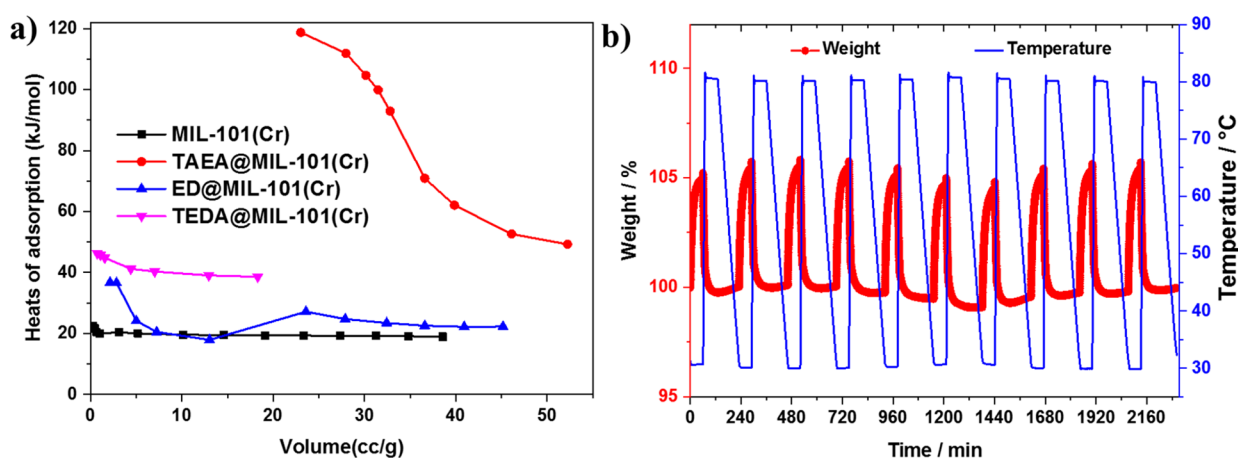


Figure 8. (a) CO₂ adsorption enthalpy curves and (b) CO₂ adsorption/desorption cycle test of TAEA@MIL-101(Cr).

K are listed in Table 1. At 1 bar and 273 K, the CO₂ adsorption capacity of TAEA@MIL-101(Cr) is up to 5.05 mmol g⁻¹, which means improvement of 54.9% compared with MIL-101(Cr). Similarly, the CO₂ adsorption capacity of ED@MIL-101(Cr) and TEDA@MIL-101(Cr) is higher than that of unmodified MIL-101. The increase of CO₂ adsorption capacity is mainly due to the chemical modification of the pore environment, which enhances the affinity of the adsorbent materials toward CO₂ molecules through dipole–quadrupole interactions.⁶¹ Combined with the EA results, sorption capacity could be utilized to obtain the molar ratio of adsorbed CO₂ to amine appended to MIL-101(Cr). As demonstrated in Table S2, at 273 K and 1.0 bar, each appended TAEA molecule adsorbs *ca.* two CO₂ molecules, while every three appended ED or TEDA molecules adsorb four CO₂ molecules. In addition, the pore modification of amine molecules can effectively reduce the pore size of the materials. It is worth noting that both TAEA@MIL-101(Cr) and ED@MIL-101(Cr) show much larger adsorption/desorption hysteresis loops than those of TEDA@MIL-101(Cr) and MIL-101(Cr), indicating the stronger intermolecular interactions between TAEA/ED molecules and CO₂. The CO₂ adsorption properties of the three materials at room temperature are similar to those at 273 K. One of the purposes of grafting organic amine molecules onto open metal sites of MIL-101(Cr) is to increase the adsorption capacity of CO₂, and most importantly the amine molecules can occupy the open metal sites of MIL-101, shifting the adsorptive sites from open Cr(III)

to amine groups, which will effectively reduce the adsorption of CO on the materials. As expected, the CO adsorption capacity of TAEA@MIL-101(Cr), ED@MIL-101(Cr) and TEDA@MIL-101(Cr) are lower than that of unmodified MIL-101(Cr) at both 273 and 298 K.

In order to illustrate the CO₂ separation performance quantitatively, the selectivity of CO₂/CO was calculated by the IAST method, based on CO₂/CO (50/50) mixture. The CO₂/CO selectivities at 273 and 298 K are shown in Figure 7. Compared with unmodified MIL-101(Cr), the selectivities of CO₂/CO of three modified MIL-101(Cr) composites increase substantially. Among them, the separation performance of TAEA@MIL-101(Cr) becomes the best, with the average (arithmetic mean of IAST selectivity from 0–1 bar) up to 508.9 at 273 K, while the averages of ED@MIL-101(Cr) and TEDA@MIL-101(Cr) are 17.3 and 15.5, respectively. And the selectivity of MIL-101(Cr) is only about 3.6. At 298 K, the CO₂/CO selectivity of TAEA@MIL-101(Cr) is the highest (857.6), but that of TEDA@MIL-101(Cr) is lower than that of MIL-101(Cr). The average CO₂ selectivity of ED@MIL-101(Cr), MIL-101(Cr) and TEDA@MIL-101(Cr) become 15.2, 8.1 and 3.7, respectively. The CO₂/CO selectivity of TAEA@MIL-101(Cr) is the highest because the introduction of TAEA molecules into MIL-101(Cr) channels could produce more adsorption sites, with primary amines and tertiary amines both involved for CO₂ uptake, leading to intensified affinity toward CO₂. While TAEA, of larger molecule size, also effectively

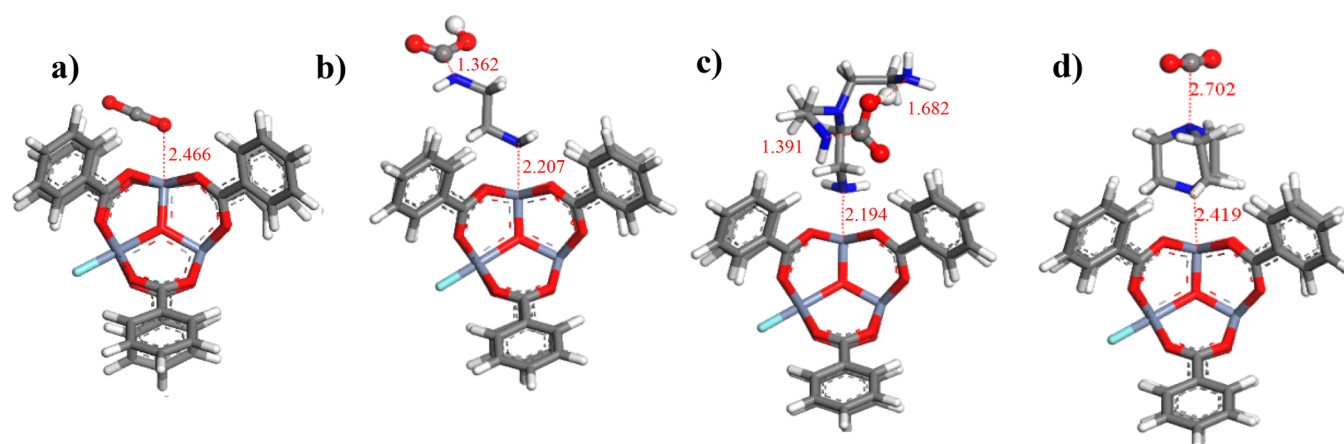


Figure 9. Structures of CO₂ adsorbed on parent and amine-grafted MIL-101(Cr).

reduce the pore aperture, so that the molecular sieving effect could be enhanced, resulting in less CO uptakes.

The pursuit of excellent solid adsorbents should not only concentrate on high capacity and high selectivity but also focus on moderate adsorption enthalpy and good reproducibility. According to the CO₂ adsorption data of 273, 293 and 298 K, the adsorption enthalpy (Q_{st}) result was obtained, which can be a quantitative understanding of the interaction strength between CO₂ and MOFs (Figure 8a). The isosteric enthalpy of three kinds of organic amine modified MIL-101(Cr) is higher than that of the original MIL-101(Cr). Besides, the adsorption enthalpy of TAEA@MIL-101(Cr) is much higher than that of the other three samples. It is mainly attributed to the strong interaction between organic amine and CO₂ and the small pore size after modification. By investigating the Q_{st} of low coverage, we can fully understand the inherent interaction strength between CO₂ and MOFs. When MIL-101(Cr) is modified by TAEA at low CO₂ coverage, Q_{st} of TAEA@MIL-101(Cr) is up to 118.7 kJ/mol. With the increase of adsorption loading, Q_{st} was down to 49.2 kJ/mol, but still higher than that of MIL-101(Cr) (22.4 kJ/mol).

As TAEA@MIL-101(Cr) has higher CO₂ adsorption enthalpy, it could be possibly difficult to regenerate theoretically. In order to test the regenerability of TAEA@MIL-101(Cr), the CO₂ adsorption and desorption cycles were performed by thermogravimetric analyzer. First of all, the sample adsorbs CO₂ at 35 °C for 60 min, and then it was purged with nitrogen gas at 80 °C for 60 min. As shown in Figure 8b, the CO₂ adsorption capacity of TAEA@MIL-101(Cr) in the ten cycles is not significantly reduced, but also has good cyclic adsorption and desorption stability.

Simulation Results. The 88-atom model with three Cr(III) have been considered (Figure 9a). Three Cr atoms of the model, as five-coordinated with O_{carboxyl} from the ligand, remain one uncoordinated site that can interact with guest molecules. The optimized geometries of the MIL-101(Cr) and amine modified MIL-101(Cr), before and after CO₂ adsorption, are presented in Figure 9.

Apparently, the adsorption site of CO₂ on MIL-101(Cr) is uncoordinated Cr(III). Partial electrons from p orbital of O_{CO₂} transfer to d_z^2 orbital of Cr(III), which leads to a weak intermolecular interaction. The O_{CO₂}-Cr(III) distance is about 2.466 Å with adsorption enthalpy of 23 kJ/mol obtained from calculation, which agreed with experimental value derived from isotherms. When amine molecules are introduced into MIL-

101(Cr), the electrons of N atom in amine transfer more readily to Cr(III) than O_{CO₂} atom because of its weaker electronegativity. When frameworks are grafted by TAEA and ED, the N-Cr(III) distance is obviously shorter than O_{CO₂}-Cr(III) distance as shown in Figure 9. Regarding TEDA, because of its steric effect caused by H atoms, the N_{TEDA}-Cr is slightly shorter than O_{CO₂}-Cr(III), along with a little distortion. All of enthalpy of three amines attached on Cr(III) are about 150 kJ/mol, indicating a strong interaction and well stability.

Compared with CO₂ adsorption on pure MIL-101(Cr), the adsorption sites have changed from Cr(III) to N atom on amine grafted MIL-101(Cr). Lone-pair electrons from sp^3 hybridized N atoms shift to C_{CO₂} atom with partial positive charge, leading to a weak intermolecular interaction. In TEDA molecule, N atoms are fully combined with three -CH₂- groups which drive electrons to focus on N atom, while on the other hand making the rigid TEDA attracting CO₂ in the conformation of linear Cr-N...N-C_{CO₂}. Such a sole and rigid interacting site would contribute very little for CO₂ capture enhancement. The simulation results shown that C_{CO₂}-N_{TEDA} distance is 2.702 Å with enthalpy as 29 kJ/mol, agreeing well with experimental results. ED and TAEA are both primary amines in which N atoms are combined with one -CH₂- group and two H atoms. Theoretically, the electrons density on N atom is lower than that on tertiary amine TEDA, leading to a longer C-N distance and a weaker molecular interaction. However, it was worth noting that both of TAEA@MIL-101(Cr) and ED@MIL-101(Cr) have much higher CO₂ uptake than TEDA@MIL-101(Cr). Especially, TAEA@MIL-101(Cr) present ultrahigh experimental heat of adsorption than others, implying absolutely adsorptive mechanism. Differing from TEDA and ED, TAEA has two flexible amine branches both with H atoms. The branches of amine groups are close enough for proton H transfer under the collaborative effect of CO₂. Thus, we proposed a plausible adsorptive mechanism as shown in Figure 9c. When adsorbed CO₂ is close to N atoms, electrons transfer from N to C and results in weakening of N-H bonds, with H atom attracted by O_{CO₂}. Under the cooperative effect of the other flexible amine group, the original N-H bond broke and formed a new N-CO₂H group which has strong interaction with the R-NH₂ group. It was observed from simulation that linear CO₂ molecules would bend upon binding with N atom. Based on this adsorptive mechanism, the calculated isosteric heat (120 kJ/mol) agrees well with the experimental value, indicating our proposed mechanism is reasonable.

Regarding ED, the distance between two grafted amines in 5- or 6-membered rings is too long to form a hydrogen bond between proton H which transfer from N atom to O atom and neighbored N atom from the other ED. The absorbed CO₂ molecules show a conformation plotted in Figure 9c. When CO₂ molecules approach the amine group, part of electrons shift from N to C atom. Meanwhile, one of the H atoms bonded with N_{amine} transports from N to O_{CO₂}. Finally, a bending HCO₂⁻ conformation formed and binded with amine through N atom. The calculated enthalpy (39 kJ/mol) agrees with experimental value very well. Thus, compared to TAEA grafted MIL-101(Cr), ED grafted MIL-101(Cr) has lower uptake and isosteric heat.

CONCLUSIONS

Three organoamine grafted MIL-101(Cr) were successfully synthesized by a double-solvent method, which indicated that this strategy is simple and efficient for the small molecule loading into MOFs. Notedly, the TAEA molecules occupy the open metal sites of MIL-101(Cr), resulting in a remarkable increase of CO₂ uptake and a substantial reduction in the sorption capacity of CO. This effective method has demonstrated a good exemplification to improve the CO₂ capacity and CO₂/CO selectivity by loading the organic amine molecules in the porous materials by the postmodification, while bringing the least impact toward parent MOFs.

ASSOCIATED CONTENT

Supporting Information

The Supporting Information is available free of charge on the ACS Publications website at DOI: 10.1021/acssuschemeng.8b03597.

TEM images of materials, breakthrough plot with syngas, elemental analysis results, detailed fitting results of CO and CO₂ sorption isotherms for pristine and three kinds of amine-modified MIL-101(Cr) with Langmuir model and calculation of gas selectivity according to IAST method (PDF)

AUTHOR INFORMATION

Corresponding Authors

*Ruiqin Zhong (rzhong@cup.edu.cn).

*Ruqiang Zou (rzou@pku.edu.cn).

ORCID

Jia Liu: 0000-0002-0892-1539

Ruqiang Zou: 0000-0003-0456-4615

Author Contributions

[§]R. Zhong, X. Yu and W. Meng contributed equally to this work.

Notes

The authors declare no competing financial interest.

ACKNOWLEDGMENTS

This work was financially supported by the National Natural Science Foundation of China (No. 51772329) and the Peking University CCUS project supported by BHP Billiton.

REFERENCES

(1) Liu, Y.; Wang, Z. U.; Zhou, H.-C. Recent advances in carbon dioxide capture with metal-organic frameworks. *Greenhouse Gases: Sci. Technol.* **2012**, *2* (4), 239–259.

(2) Solomon, S.; Plattner, G. K.; Knutti, R.; Friedlingstein, P. Irreversible climate change due to carbon dioxide emissions. *Proc. Natl. Acad. Sci. U. S. A.* **2009**, *106* (6), 1704–1709.

(3) Feely, R.; Doney, S.; Cooley, S. Ocean Acidification: Present Conditions and Future Changes in a High-CO₂ World. *Oceanography* **2009**, *22* (4), 36–47.

(4) Rao, A. B.; Rubin, E. S. A technical, economic, and environmental assessment of amine-based CO₂ capture technology for power plant greenhouse gas control. *Environ. Sci. Technol.* **2002**, *36* (20), 4467–75.

(5) Haszeldine, R. S. Carbon capture and storage: how green can black be? *Science* **2009**, *325* (5948), 1647–1652.

(6) Hagewiesche, D. P.; Ashour, S. S.; Al-Ghawas, H. A.; Sandall, O. C. Absorption of carbon dioxide into aqueous blends of monoethanolamine and N-methyldiethanolamine. *Chem. Eng. Sci.* **1995**, *50* (7), 1071–1079.

(7) David, J. *Economic Evaluation of Leading Technology Options for Sequestration of Carbon Dioxide*; Massachusetts Institute of Technology: Boston, MA, 2000.

(8) Meratla, Z. Combining cryogenic flue gas emission remediation with a combustion cycle. *Energy Convers. Manage.* **1997**, *38*, S147–S152.

(9) Zhao, L.; Riensche, E.; Menzer, R.; Blum, L.; Stolten, D. A parametric study of CO₂/N₂ gas separation membrane processes for post-combustion capture. *J. Membr. Sci.* **2008**, *325* (1), 284–294.

(10) Demontigny, D.; Tontiwachwuthikul, P.; Chakma, A. Using polypropylene and polytetrafluoroethylene membranes in a membrane contactor for CO₂ absorption. *J. Membr. Sci.* **2006**, *277* (1–2), 99–107.

(11) Bounaceur, R.; Lape, N.; Roizard, D.; Vallieres, C.; Favre, E. Membrane processes for post-combustion carbon dioxide capture: A parametric study. *Energy* **2006**, *31* (14), 2556–2570.

(12) Li, J.-R.; Ma, Y.; McCarthy, M. C.; Sculley, J.; Yu, J.; Jeong, H.-K.; Balbuena, P. B.; Zhou, H.-C. Carbon dioxide capture-related gas adsorption and separation in metal-organic frameworks. *Coord. Chem. Rev.* **2011**, *255* (15–16), 1791–1823.

(13) D'Alessandro, D. M.; Smit, B.; Long, J. R. Carbon Dioxide Capture: Prospects for New Materials. *Angew. Chem., Int. Ed.* **2010**, *49* (35), 6058–6082.

(14) Choi, S.; Drese, J. H.; Jones, C. W. Adsorbent materials for carbon dioxide capture from large anthropogenic point sources. *ChemSusChem* **2009**, *2* (9), 796–854.

(15) McEwen, J.; Hayman, J.-D.; Ozgur Yazaydin, A. A comparative study of CO₂, CH₄ and N₂ adsorption in ZIF-8, Zeolite-13X and BPL activated carbon. *Chem. Phys.* **2013**, *412*, 72–76.

(16) Ferey, G.; Serre, C.; Devic, T.; Maurin, G.; Jobic, H.; Llewellyn, P. L.; De Weireld, G.; Vimont, A.; Daturi, M.; Chang, J. S. Why hybrid porous solids capture greenhouse gases? *Chem. Soc. Rev.* **2011**, *40* (2), 550–562.

(17) Furukawa, H.; Cordova, K. E.; O'Keeffe, M.; Yaghi, O. M. The chemistry and applications of metal-organic frameworks. *Science* **2013**, *341* (6149), 1230444.

(18) Mueller, U.; Schubert, M.; Teich, F.; Puetter, H.; Schierle-Arndt, K.; Pastré, J. Metal-organic frameworks—prospective industrial applications. *J. Mater. Chem.* **2006**, *16* (7), 626–636.

(19) Ferey, G.; Serre, C. Large breathing effects in three-dimensional porous hybrid matter: facts, analyses, rules and consequences. *Chem. Soc. Rev.* **2009**, *38* (5), 1380–1399.

(20) Britt, D.; Furukawa, H.; Wang, B.; Glover, T. G.; Yaghi, O. M. Highly efficient separation of carbon dioxide by a metal-organic framework replete with open metal sites. *Proc. Natl. Acad. Sci. U. S. A.* **2009**, *106* (49), 20637–20640.

(21) An, J.; Geib, S. J.; Rosi, N. L. High and selective CO₂ uptake in a cobalt adeninate metal-organic framework exhibiting pyrimidine- and amino-decorated pores. *J. Am. Chem. Soc.* **2010**, *132* (1), 38–39.

(22) Bae, Y. S.; Snurr, R. Q. Development and evaluation of porous materials for carbon dioxide separation and capture. *Angew. Chem., Int. Ed.* **2011**, *50* (49), 11586–11596.

(23) Zhang, Z.; Zhao, Y.; Gong, Q.; Li, Z.; Li, J. MOFs for CO₂ capture and separation from flue gas mixtures: the effect of

multifunctional sites on their adsorption capacity and selectivity. *Chem. Commun.* **2013**, 49 (7), 653–661.

(24) Ferey, G. Hybrid porous solids: past, present, future. *Chem. Soc. Rev.* **2008**, 37 (1), 191–214.

(25) Banerjee, R.; Phan, A.; Wang, B.; Knobler, C.; Furukawa, H.; O’Keeffe, M.; Yaghi, O. M. High-throughput synthesis of zeolitic imidazolate frameworks and application to CO₂ capture. *Science* **2008**, 319 (5865), 939–943.

(26) Deng, H.; Grunder, S.; Cordova, K. E.; Valente, C.; Furukawa, H.; Hmadeh, M.; Gandara, F.; Whalley, A. C.; Liu, Z.; Asahina, S.; Kazumori, H.; O’Keeffe, M.; Terasaki, O.; Stoddart, J. F.; Yaghi, O. M. Large-pore apertures in a series of metal-organic frameworks. *Science* **2012**, 336 (6084), 1018–1023.

(27) An, J.; Rosi, N. L. Tuning MOF CO₂ adsorption properties via cation exchange. *J. Am. Chem. Soc.* **2010**, 132 (16), 5578–5579.

(28) Park, H. J.; Cheon, Y. E.; Suh, M. P. Post-synthetic reversible incorporation of organic linkers into porous metal-organic frameworks through single-crystal-to-single-crystal transformations and modification of gas-sorption properties. *Chem. - Eur. J.* **2010**, 16 (38), 11662–11669.

(29) Xiang, Z.; Hu, Z.; Cao, D.; Yang, W.; Lu, J.; Han, B.; Wang, W. Metal-organic frameworks with incorporated carbon nanotubes: improving carbon dioxide and methane storage capacities by lithium doping. *Angew. Chem., Int. Ed.* **2011**, 50 (2), 491–494.

(30) Choi, S.; Watanabe, T.; Bae, T. H.; Sholl, D. S.; Jones, C. W. Modification of the Mg/DOBDC MOF with Amines to Enhance CO₂ Adsorption from Ultradilute Gases. *J. Phys. Chem. Lett.* **2012**, 3 (9), 1136–1141.

(31) Huang, Y.; Qin, W.; Li, Z.; Li, Y. Enhanced stability and CO₂ affinity of a UiO-66 type metal-organic framework decorated with dimethyl groups. *Dalton Trans* **2012**, 41 (31), 9283–9285.

(32) Buragohain, A.; Van Der Voort, P.; Biswas, S. Facile synthesis and gas adsorption behavior of new functionalized Al-MIL-101-X (X = –CH₃, –NO₂, –OCH₃, –C₆H₄, –F₂, –(CH₃)₂, –(OCH₃)₂) materials. *Microporous Mesoporous Mater.* **2015**, 215, 91–97.

(33) Frysali, M. G.; Klontzas, E.; Tylianakis, E.; Froudakis, G. E. Tuning the interaction strength and the adsorption of CO₂ in metal organic frameworks by functionalization of the organic linkers. *Microporous Mesoporous Mater.* **2016**, 227, 144–151.

(34) Huang, H.; Zhang, W.; Yang, F.; Wang, B.; Yang, Q.; Xie, Y.; Zhong, C.; Li, J.-R. Enhancing CO₂ adsorption and separation ability of Zr(IV)-based metal-organic frameworks through ligand functionalization under the guidance of the quantitative structure–property relationship model. *Chem. Eng. J.* **2016**, 289, 247–253.

(35) Wang, D.; Wang, Z.; Wang, L.; Hu, L.; Jin, J. Ultrathin membranes of single-layered MoS₂ nanosheets for high-permeance hydrogen separation. *Nanoscale* **2015**, 7 (42), 17649–17652.

(36) Chen, Z.; Deng, S.; Wei, H.; Wang, B.; Huang, J.; Yu, G. Polyethylenimine-impregnated resin for high CO₂ adsorption: an efficient adsorbent for CO₂ capture from simulated flue gas and ambient air. *ACS Appl. Mater. Interfaces* **2013**, 5 (15), 6937–6945.

(37) Zhang, Z.; Xian, S.; Xia, Q.; Wang, H.; Li, Z.; Li, J. Enhancement of CO₂ Adsorption and CO₂/N₂ Selectivity on ZIF-8 via Postsynthetic Modification. *AIChE J.* **2013**, 59 (6), 2195–2206.

(38) Cogswell, C. F.; Jiang, H.; Ramberger, J.; Accetta, D.; Willey, R. J.; Choi, S. Effect of Pore Structure on CO₂ Adsorption Characteristics of Aminopolymer Impregnated MCM-36. *Langmuir* **2015**, 31 (15), 4534–4541.

(39) Yeon, J. S.; Lee, W. R.; Kim, N. W.; Jo, H.; Lee, H.; Song, J. H.; Lim, K. S.; Kang, D. W.; Seo, J. G.; Moon, D.; Wiers, B.; Hong, C. S. Homodiamine-functionalized metal-organic frameworks with a MOF-74-type extended structure for superior selectivity of CO₂ over N₂. *J. Mater. Chem. A* **2015**, 3 (37), 19177–19185.

(40) Martínez, F.; Sanz, R.; Orcajo, G.; Briones, D.; Yáñez, V. Amino-impregnated MOF materials for CO₂ capture at post-combustion conditions. *Chem. Eng. Sci.* **2016**, 142, 55–61.

(41) Anbia, M.; Hoseini, V. Enhancement of CO₂ adsorption on nanoporous chromium terephthalate (MIL-101) by amine modification. *J. Nat. Gas Chem.* **2012**, 21 (3), 339–343.

(42) Andirova, D.; Lei, Y.; Zhao, X.; Choi, S. Functionalization of Metal-Organic Frameworks for Enhanced Stability under Humid Carbon Dioxide Capture Conditions. *ChemSusChem* **2015**, 8 (20), 3405–3409.

(43) Li, L.-J.; Liao, P.-Q.; He, C.-T.; Wei, Y.-S.; Zhou, H.-L.; Lin, J.-M.; Li, X.-Y.; Zhang, J.-P. Grafting alkylamine in UiO-66 by charge-assisted coordination bonds for carbon dioxide capture from high-humidity fluid gas. *J. Mater. Chem. A* **2015**, 3 (43), 21849–21855.

(44) Ferey, G.; Mellot-Draznieks, C.; Serre, C.; Millange, F.; Dutour, J.; Surble, S.; Margiolaki, I. A chromium terephthalate-based solid with unusually large pore volumes and surface area. *Science* **2005**, 309 (5743), 2040–2042.

(45) Hwang, Y. K.; Hong, D. Y.; Chang, J. S.; Jhung, S. H.; Seo, Y. K.; Kim, J.; Vimont, A.; Daturi, M.; Serre, C.; Ferey, G. Amine grafting on coordinatively unsaturated metal centers of MOFs: consequences for catalysis and metal encapsulation. *Angew. Chem., Int. Ed.* **2008**, 47 (22), 4144–8.

(46) Hong, D.-Y.; Hwang, Y. K.; Serre, C.; Férey, G.; Chang, J.-S. Porous Chromium Terephthalate MIL-101 with Coordinatively Unsaturated Sites: Surface Functionalization, Encapsulation, Sorption and Catalysis. *Adv. Funct. Mater.* **2009**, 19 (10), 1537–1552.

(47) Anjum, M. W.; Vermoortele, F.; Khan, A. L.; Bueken, B.; De Vos, D. E.; Vankelecom, I. F. Modulated UiO-66-Based Mixed-Matrix Membranes for CO₂ Separation. *ACS Appl. Mater. Interfaces* **2015**, 7 (45), 25193–25201.

(48) Huang, Y.; Xiao, Y.; Huang, H.; Liu, Z.; Liu, D.; Yang, Q.; Zhong, C. Ionic liquid functionalized multi-walled carbon nanotubes/zeolitic imidazolate framework hybrid membranes for efficient H₂/CO₂ separation. *Chem. Commun.* **2015**, 51 (97), 17281–4.

(49) Darunte, L. A.; Oetomo, A. D.; Walton, K. S.; Sholl, D. S.; Jones, C. W. Direct Air Capture of CO₂ Using Amine Functionalized MIL-101(Cr). *ACS Sustainable Chem. Eng.* **2016**, 4 (10), 5761–5768.

(50) Lin, Y.; Lin, H.; Wang, H.; Suo, Y.; Li, B.; Kong, C.; Chen, L. Enhanced selective CO₂ adsorption on polyamine/MIL-101(Cr) composites. *J. Mater. Chem. A* **2014**, 2 (35), 14658–14665.

(51) Serra-Crespo, P.; Ramos-Fernandez, E. V.; Gascon, J.; Kapteijn, F. Synthesis and Characterization of an Amino Functionalized MIL-101(Al): Separation and Catalytic Properties. *Chem. Mater.* **2011**, 23 (10), 2565–2572.

(52) Wang, X.; Li, H.; Hou, X.-J. Amine-Functionalized Metal Organic Framework as a Highly Selective Adsorbent for CO₂ over CO. *J. Phys. Chem. C* **2012**, 116 (37), 19814–19821.

(53) Hu, Y.; Verdegaal, W. M.; Yu, S. H.; Jiang, H. L. Alkylamine-tethered stable metal-organic framework for CO₂ capture from flue gas. *ChemSusChem* **2014**, 7 (3), 734–737.

(54) Li, H.; Wang, K.; Feng, D.; Chen, Y. P.; Verdegaal, W.; Zhou, H. C. Incorporation of Alkylamine into Metal-Organic Frameworks through a Bronsted Acid-Base Reaction for CO₂ Capture. *ChemSusChem* **2016**, 9 (19), 2832–2840.

(55) Aijaz, A.; Karkamkar, A.; Choi, Y. J.; Tsumori, N.; Ronnebro, E.; Autrey, T.; Shioyama, H.; Xu, Q. Immobilizing highly catalytically active Pt nanoparticles inside the pores of metal-organic framework: a double solvents approach. *J. Am. Chem. Soc.* **2012**, 134 (34), 13926–13929.

(56) Bromberg, L.; Diao, Y.; Wu, H.; Speakman, S. A.; Hatton, T. A. Chromium(III) Terephthalate Metal Organic Framework (MIL-101): HF-Free Synthesis, Structure, Polyoxometalate Composites, and Catalytic Properties. *Chem. Mater.* **2012**, 24 (9), 1664–1675.

(57) Xing, B.; Pignatello, J. J.; Gigliotti, B. Competitive Sorption between Atrazine and Other Organic Compounds in Soils and Model Sorbents. *Environ. Sci. Technol.* **1996**, 30 (8), 2432–2440.

(58) Kong, L.; Zou, R.; Bi, W.; Zhong, R.; Mu, W.; Liu, J.; Han, R. P. S.; Zou, R. Selective adsorption of CO₂/CH₄ and CO₂/N₂ within a charged metal-organic framework. *J. Mater. Chem. A* **2014**, 2 (42), 17771–17778.

(59) Goerigk, L.; Grimme, S. A thorough benchmark of density functional methods for general main group thermochemistry, kinetics, and noncovalent interactions. *Phys. Chem. Chem. Phys.* **2011**, 13 (14), 6670–6688.

(60) Adamo, C.; Barone, V. Toward reliable density functional methods without adjustable parameters: The PBE0 model. *J. Chem. Phys.* **1999**, *110* (13), 6158–6170.

(61) Zheng, B.; Bai, J.; Duan, J.; Wojtas, L.; Zaworotko, M. J. Enhanced CO₂ binding affinity of a high-uptake rht-type metal-organic framework decorated with acylamide groups. *J. Am. Chem. Soc.* **2011**, *133* (4), 748–751.